General Disclaimer

One or more of the Following Statements may affect this Document

- This document has been reproduced from the best copy furnished by the organizational source. It is being released in the interest of making available as much information as possible.

- This document may contain data, which exceeds the sheet parameters. It was furnished in this condition by the organizational source and is the best copy available.

- This document may contain tone-on-tone or color graphs, charts and/or pictures, which have been reproduced in black and white.

- This document is paginated as submitted by the original source.

- Portions of this document are not fully legible due to the historical nature of some of the material. However, it is the best reproduction available from the original submission.

Electrical Engineering Department
UNIVERSITY OF MARYLAND, COLLEGE PARK, MD 20742

Semi-annual Technical Report

The Study of Surface Acoustic Wave Charge Transfer Device

for

NASA Research Grant No. NSG 1468

Grant Monitor: Dr. H. F. Benz
Flight Electronic Division
Langley Research Center
Hampton, Va. 23665

Prepared by:

N. Papanicolaou and H. C. Lin
Electrical Engineering Department
University of Maryland
College Park, Maryland 20742

July 13, 1978

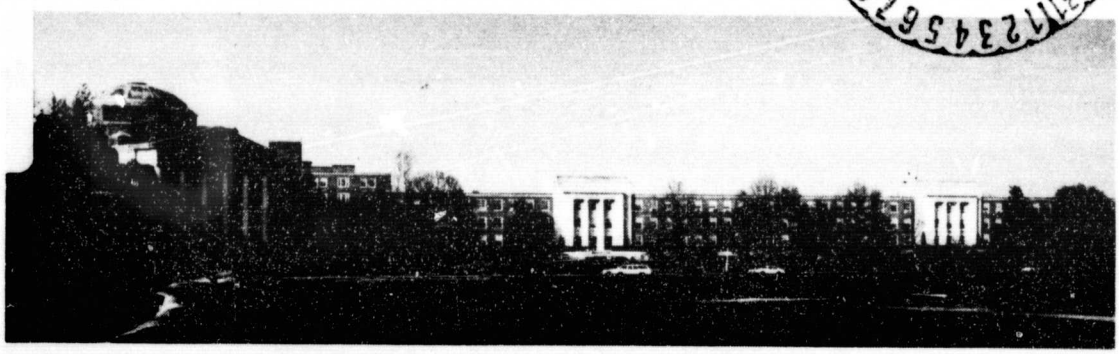

COLLEGE OF ENGINEERING: GLENN L. MARTIN INSTITUTE OF TECHNOLOGY

Semi-annual Technical Report

The Study of Surface Acoustic Wave Charge Transfer Device

for

NASA Research Grant No. NSG 1468

Grant Monitor: Dr. H. F. Benz
Flight Electronic Division
Langley Research Center
Hampton, Va. 23665

Prepared by:

N. Papanicolaou and H. C. Lin
Electrical Engineering Department
University of Maryland
College Park, Maryland 20742

July 13, 1978

Surface Acoustic Wave Charge Transfer Device

Introduction

In recent years the charge-coupled device is creating a great deal of interest for applications in memory, signal processing and imaging. The incentive for the interest lies in the simplicity in structure and high density. However, the CCD technology has a number of drawbacks which limit the density, the speed and the processing simplicity. For instance, (in a typical CCD structure as shown in Fig. 1, three or four phase clocks are required to transfer the charges; multilevel metalization is required to effect the multi-phase clocks; buried channel is required to improve the speed; and for imagers, separate charge storage and transfer areas must be provided because of the masking of the clock busses. This work is a study of the possibility of circumventing these problems of the CCD by use of surface acoustic waves.

In the proposed device, surface acoustic waves are used to create traveling longitudinal electric fields in the silicon and to replace the multiphase clocks of CCD. The traveling electric fields create potential wells which will carry along charges that may be stored in the wells as shown in Fig. 2. The charges may be injected into the wells by light or using a p-n junction as in a conventional CCD.

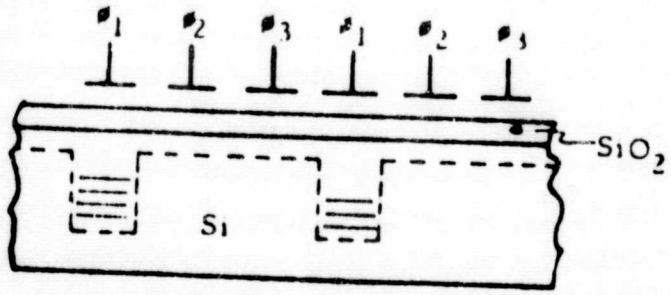

Fig. 1 The CCD

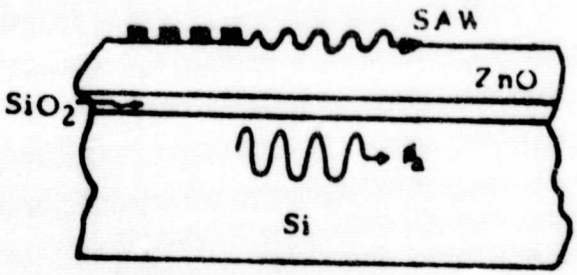

Fig. 2 Traveling SAW

Optimum Transducer Configurations:

The structure of the SAW-CTD, as proposed, consists of an n-type silicon substrate, a thermally grown silicon dioxide layer and a sputtered film of piezoelectric ZnO.

The first objective of the study of the SAW-CTD is to find the optimum conditions and structure dimensions which produce the highest piezoelectric potential at the Si-SiO_2 interface. This potential is directly proportional to $\Delta V/V$ which is the fractional velocity change of the surface acoustic wave when a shorting plane is assumed at the position of the transducer.

In order to carry out this analysis a surface acoustic wave computer program[1] was used. This program, which can be applied to a multilayer structure, was designed to calculate the velocity of the surface acoustic wave as well as the electrical and mechanical quantities associated with it.

The results obtained so far indicate that a transducer placed on top of the ZnO film with a short metal film placed directly underneath is the optimum configuration for maximum effective coupling. For a SiO_2 layer of 1000Å this maximum is $(\Delta V/V)\% = .51$ and occurs at a ZnO thickness $h = .05\lambda$ (see attached computer curves). It was also found that as the SiO_2 thickness is reduced while the thickness of the ZnO is kept constant, the effective coupling is also reduced. However, the thickness of the SiO_2 must be more than 1000Å since the potential associated with the surface acoustic wave decays exponentially with depth.

Figure 3 shows the four possible transducer configurations studied. The attached curves correspond to the variation of $\Delta V/V$ with the normalized ZnO film thickness for these configurations. **(See Figure 4)**

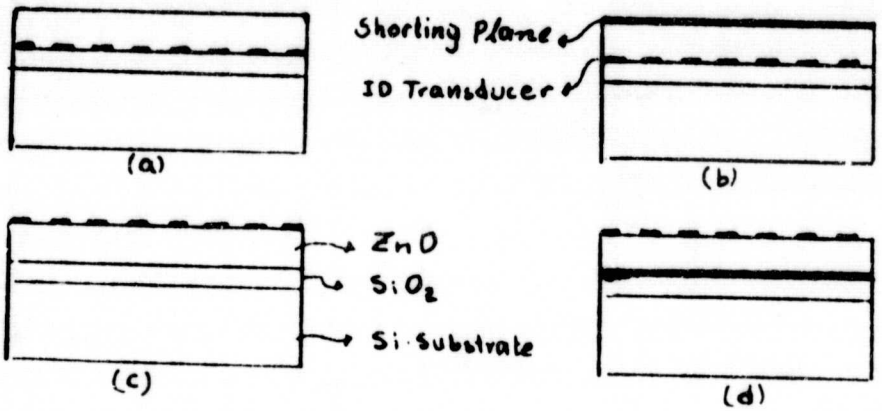

FIG 3. Four possible transducer configurations for the excitation of surface acoustic waves.

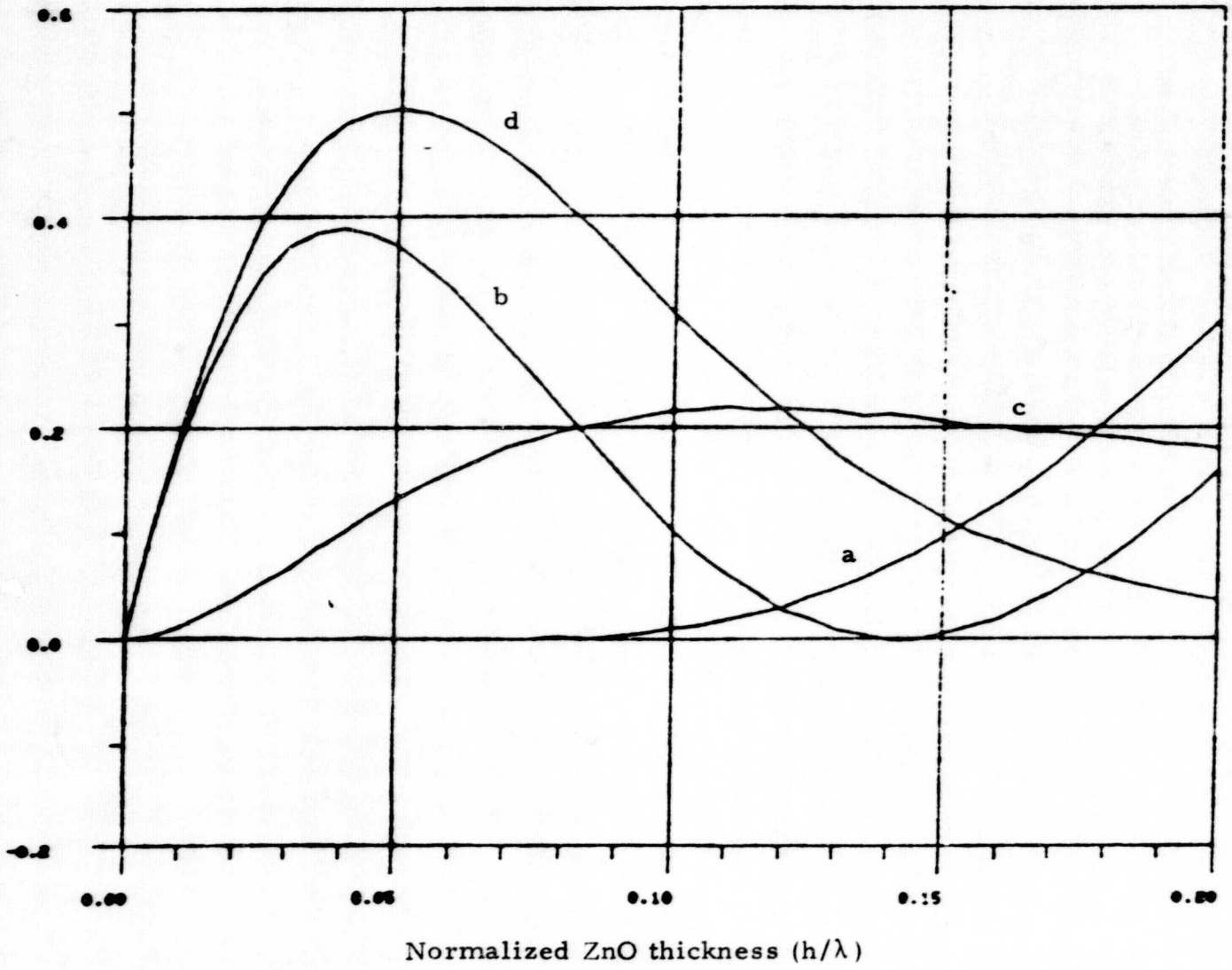

Figure 4. Percent change in velocity vs. normailized ZnO film thickness for the four transducer configuration shown in Fig. 3.

Charge Stability in the SAW-CTD

When a surface acoustic wave is propagating in the SAW-CTD structure, it produces a surface potential $\phi_{as} = \phi_0 \cos(kx-\omega t)$ at the Si-SiO_2 interface. This potential travels synchronously with the surface wave at the constant velocity $v = \lambda f = \omega/k$. This velocity, as calculated by the SAW Program, is given by the dispersion curve which is attached.

A signal charge being transferred by a potential well created by the above potential must move synchronously with the same velocity v under the influence of an electric field E_s. The analysis reveals that for a stable charge packet to exist in the well the parameter $A = \lambda v/2\pi\mu_s\phi_0$ must be less than unity. Here λ and v correspond to the wavelength and velocity of the surface acoustic wave respectively, μ_s is the minority carrier mobility of the signal charge in Si and ϕ_0 is amplitude of the acoustoelectric potential. As the value of A decreases the amount of charge that can be held in the well increases, thus improving the signal handling capability of the device.

As it may be seen from the dispersion curve, the velocity v has very little flexibility in adjusting the value of A once the ZnO thickness is chosen. If electrons are chosen as the signal charge carriers instead of holes it would result in a lower value of A, because the electron mobility is higher than that of the holes. It is also obvious that the higher the amplitude ϕ_0 of the acousto-electric potential, the lower A would be, thus higher capability. This justifies our effort to maximize the effective piezoelectric coupling for the structure as discussed previously.

Injection and capture in the SAW-CTD

Two requirements must be met in order to successfully transfer charge in a SAW-CTD. First the electric field associated with the traveling wave potential must have a tangential component along the direction of propagation. Second the velocity of the charge packet must be close to the phase velocity of the traveling wave i.e. the traveling wave and the charge packet must move in a synchronous manner.

Several techniques are used for injecting the signal charge into a Charge Transfer Device. The simplest one is by direct electrical injection of a reverse biased diode. Here, injected charge is proportional to the test signal applied to

the reverse biased diode. Another method which is useful for solid state imaging application is by photoelectric injection process in the silicon. In this case the amount of charge that is injected into a well is a function of the integrated light flux, and the device can thus be used for image sensing purposes. Since the capture of the charge in the SAW-CTD must result to a synchronous motion, the injection of charge must meet certain conditions. It can be shown that for capture to take place in the SAW-CTD the initial injection velocities of the carriers v_o must satisfy the following condition:

$$\beta_{o\,min} < \beta_o < \beta_{o\,max}$$

where:

$\beta_o = v_o / v_a$ is the normalized initial velocity of the carrier with respect to the SAW velocity denoted by v_a.

$$\beta_{o\,min} = \sqrt{\frac{4e\phi_o}{m^* v_a^2}}$$

$$\beta_{o\,max} \sqrt{\frac{4e\phi_o}{m^* v_a^2}}$$

and where

ϕ_o is the amplitude of the acoustoelectric potential, e is the electronic charge and m^* is the effective mass of the carriers.

For a typical device, where electrons are the carriers, $m_e^* = 1.09 m_e$, $v_a = 4400$m/sec and assuming $\phi_o = 1$ volt the above capture limits become

$$-8 \times 10^5 \text{ m/sec} < v_o < 8 \times 10^5 \text{ m/sec}$$

The minus sign indicates velocities opposite to the direction of the wave propagation. This means that carriers injected with velocities within the above range will be captured by the traveling wave otherwise they will be lost. Since

the above velocities are comparable to the thermal velocities of the carriers ($\sim 10^5$ m/sec at room temperature) it is possible for thermally generated carriers to be captured and transferred by the traveling electroacoustic potential. This result shows that efficient imaging devices can be made with the SAW-CTD, since most of the optically generated carriers have typical thermal velocities and will be captured by the traveling wave.

The Acoustoelectric Potential in the SAW-CTD Structure

In a previous section, it was mentioned that the transducer configurations (b) and (d) (see Fig. 3) provide maximum piezoelectric coupling for the excitation of the surface acoustic waves in the SAW-CTD structure. The peaks for these two configurations occur for a ZnO thickness of approximately .05λ.

However in the propagation region (or charge transfer region) we are looking for conditions which would produce the maximum electric potential strength at the Si surface where the charge transfer takes place. The SAW Computer Program was used again for the calculation of the variation of the electric potential with depth. In Fig. 5 and 6 the amplitude of the electric potential is normalized with respect to the amplitude of the shear displacement at the free surface. For a free non-metallized surface the electric potential decays exponentially with depth resulting to a low value at the Si surface (see Fig. 5). However when the free surface is shorted with a thin metallic film the potential at the free surface is clamped to zero, all the electrostatic energy normally stored above the free surface is now forced into the structure resulting in an increase of the potential ϕ with depth and a high value at the surface of the silicon.

Therefore, the gate electrode placed on top of the SAW-CTD structure directly over the region of charge transfer serves two

functions: first, by applying a bias to the electrode we can balance out the effect of surface states and to induce the deep depletion of the Si surface which is necessary for charge transfer, and secondly, the presence of the electrode increases the acoustoelectric potential at the silicon surface as it was shown above.

What now remains to be examined is the thickness of the insulating SiO_2 layer. Since the energy of the surface acoustic wave is concentrated inside the piezoelectric film it is obvious that as the thickness of the SiO_2 layer is increased the Si surface is moved away from the ZnO film and therefore the potential would be reduced. This effect is shown in Fig. 6 where the curves represent ϕ for various SiO_2 thicknesses. The second discontinuity of each curve corresponds to the electric potential at the Si surface. Constructing the dashed line through these discontinuities gives the value of ϕ at the Si surface as a function of the SiO_2 thickness. The variation is an exponential decay. Therefore we conclude that the thickness of the SiO_2 layer should be kept at a minimum in order that the Si surface is as close to the proximity of the ZnO film as possible, but thick enough as to avoid shorting through pin-holes in the insulating SiO_2. The thickness that would meet these requirements and also be compatible with MOS and CCD technology is approximately 1,000Å.

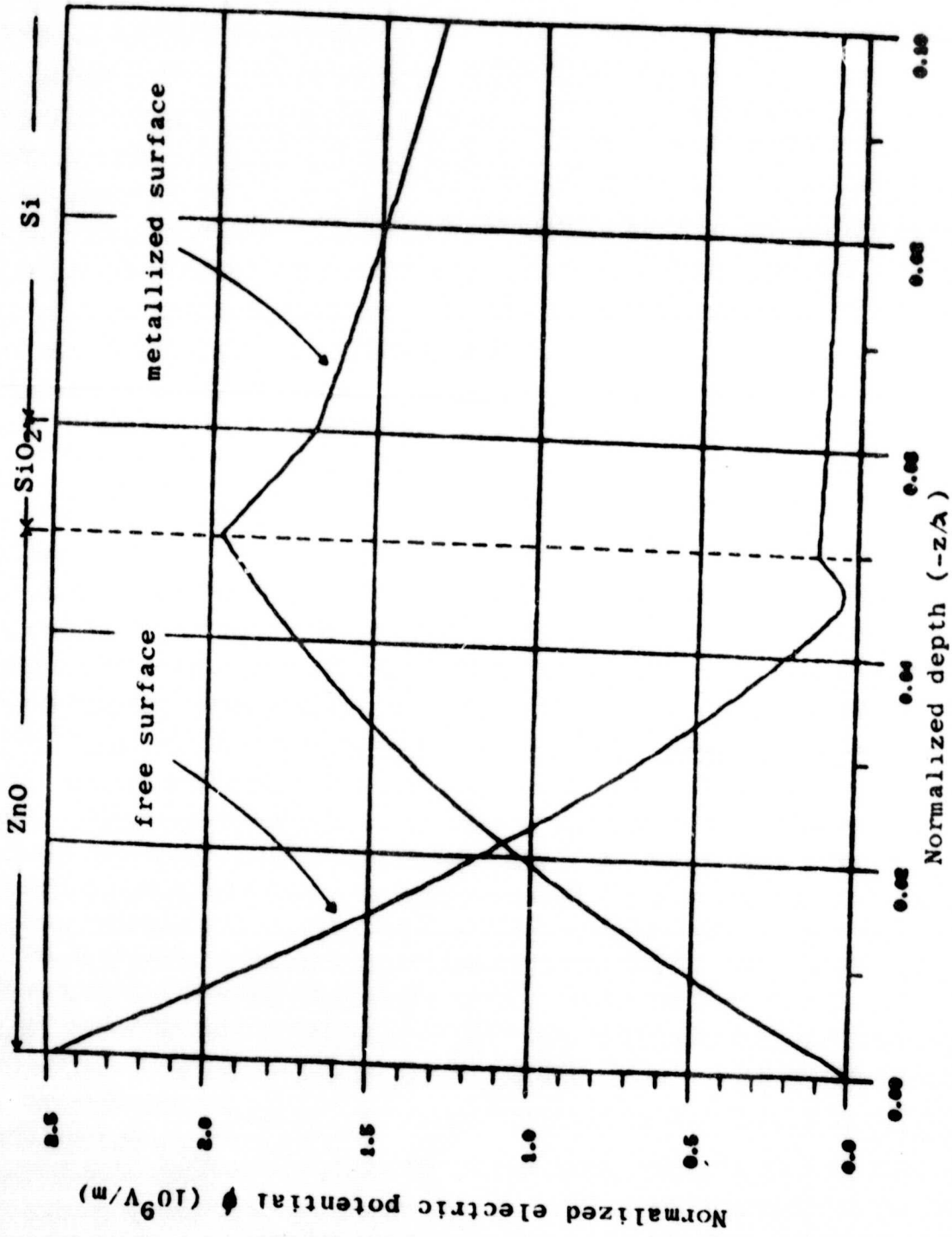

Fig 5. Electric potential vs depth for free and metallized ZnO surfaces.

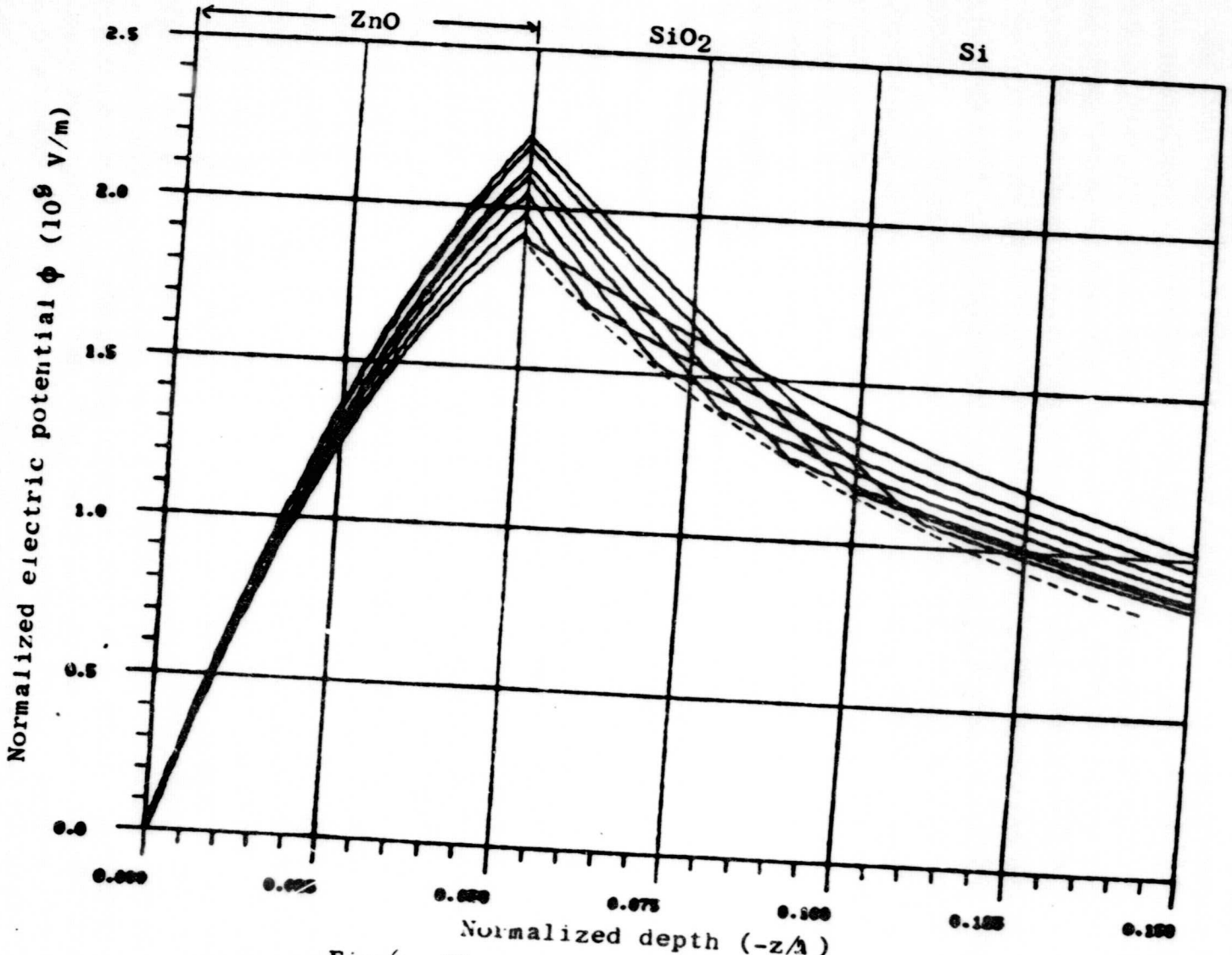

Fig 6. The spacial variation of the electric potential for various SiO_2 film thicknesses.

ZnO Film Deposition

Several methods may be used to deposit thin piezoelectric films including compound or elemental evaporation and RF reactive or compound sputtering. The RF compound sputtering of piezoelectric films is presently the most commonly used technique and reveals the best results for films intended for surface acoustic waves. A schematic diagram of the RF sputtering apparatus is shown in Fig. 7. The output of the transmitter oscillator is fed into a 2 kW power amplifier and in turn its output is supplied to the load through a matching network. Since the impedance of the glow discharge is very large, and the matching network can match loads in the range of 20-2,000Ω, a coil is used to reduce the effective load impedance to a value within the range of the Match-Box. The purpose of the large capacitor is to block the negative D.C. bias developed at the cathode. This D.C. self bias is very essential in the sputtering operation.

The system is initially purged to a pressure of 10^{-6} torr, then a mixture of 80% Argon and 20% Oxygen is admitted to the bell-jar through a precision leak-valve. Sputtering pressures are sustained in the 5-15 micron range. When the RF voltage is applied across the electrodes which are separated by a distance of 3-4 cm a glow discharge is initiated and sputtering takes place. Deposition rates of .25-.5μm per hour are obtained depending on the rf power delivered. The electrode assemblies for our sputtering system is shown in Fig. 8. The cathode plate (copper) where the ZuO target is placed, is water-cooled. The anode which supports the substrate holder is also provided with a cooling coil and a heater and its temperature is monitored through a termo-couple gauge.

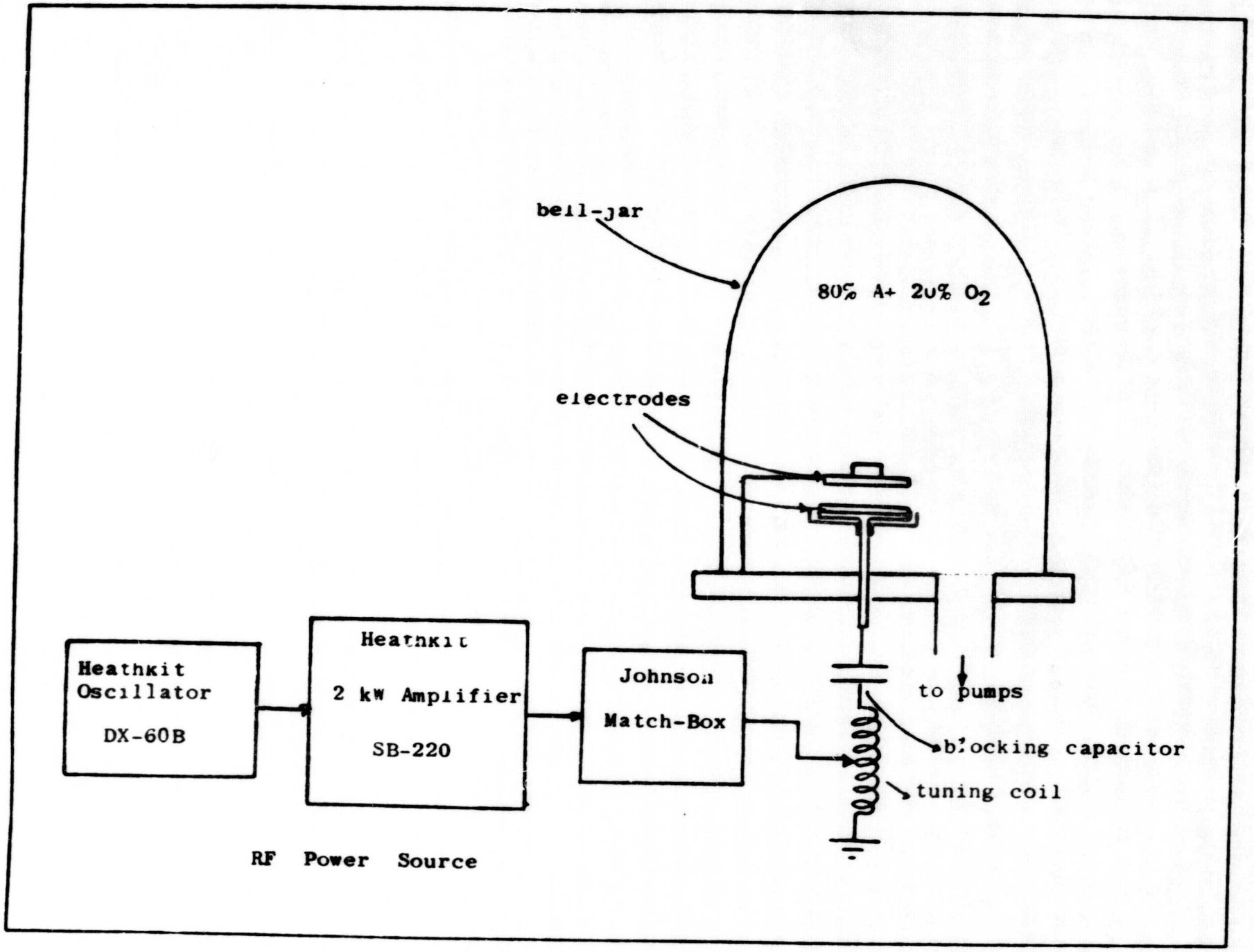

Fig 7. The RF Sputtering Apparatus.

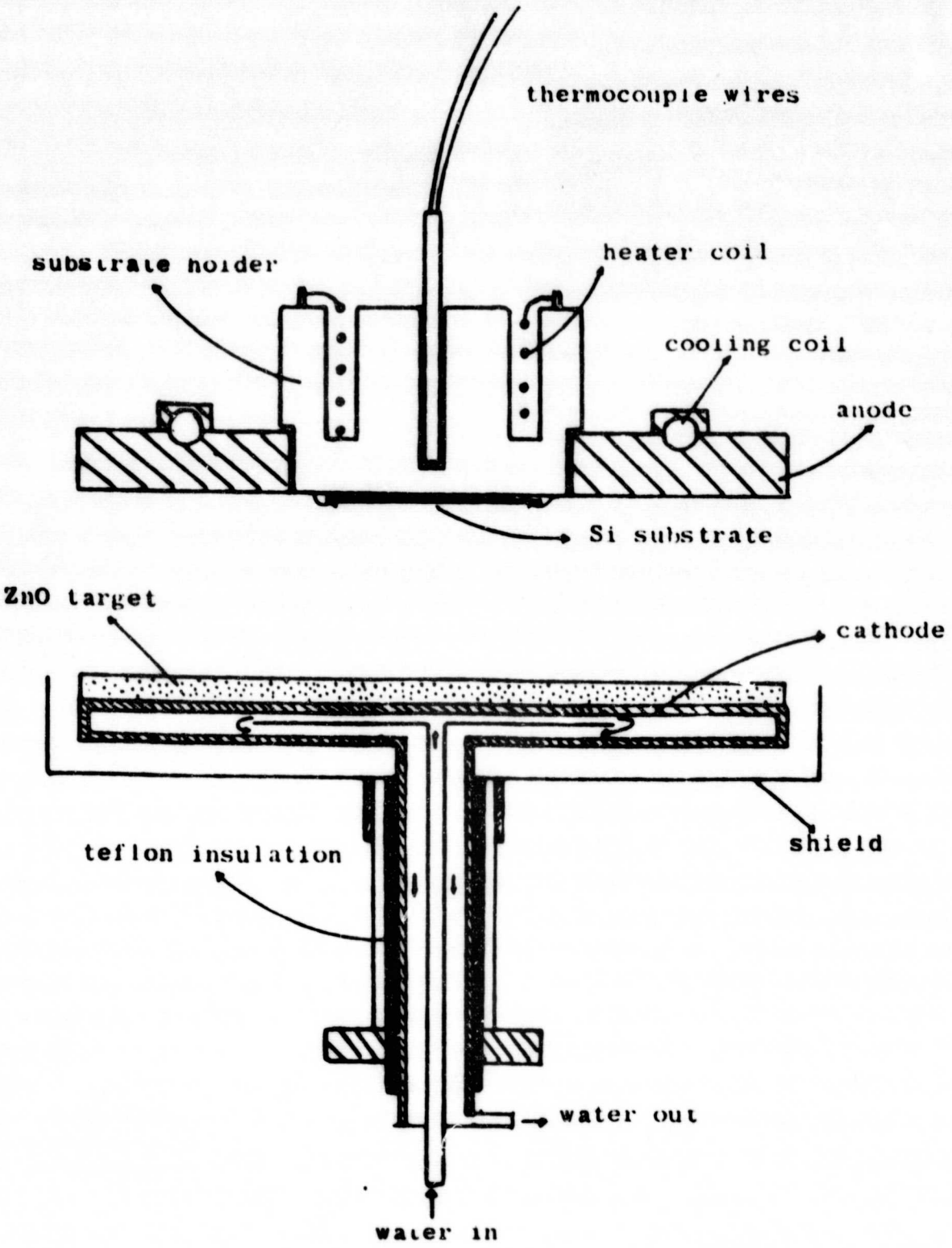

Fig. 8. Electrode Assemblies.

Check of C-Axis Orientation

The crystal orientation of the ZuO film plays a very important role in the physical properties of the film, especially if it is to be used for the excitation of surface acoustic waves. For the case of the interdigital transducer the crystallographic orientation of the film determines electromechanical constant k and thus the piezoelectric coupling efficiency of the transducer. In addition it is also related to the fractional velocity charge $\Delta V/V$ (which was discussed in earlier reports) through the expression

$$\frac{\Delta V}{V} = \frac{1}{2} k^2$$

If a ZnO film is to be used for efficiently exciting surface acoustic waves the C-axis must lie perpendicular to the substrate surface. Several methods may be used to determine the crystal orientation of the ZnO films, among them X-Ray Diffraction or Reflection Electron Diffraction (RED). A more recent technique is the examination of the sputtered films under a Scanning Electron Microscope (SEM). With this method a microscopic view of the structure of the film can be obtained at magnifications from 2,000 to 25,000. The sample is fractured or etched so that it can be viewed in cross-section, then it is coated with a thin (100 Å) film of Gold-Palladium alloy to make it electrically conductive for higher resolution. The specimen is viewed at an angle of 45°-50°. The microstructures of three ZnO films sputtered in our system are shown in Fig. 9. The most obvious physical features of these films is the columnar growth and the relatively large crystallites (200-500Å in diameter) which are densely parked. The best oriented ZnO film with high coupling coefficient is that grown on Au (Fig. 9a) whereas the film deposited on Si is poorly oriented

with grains partially disordered and thus displaying less coupling coefficient. The film grown on SiO_2 is fairly oriented. These results indicate that the crystal-structure of the substrate material has a great effect on the manner in which the ZnO film grows.

The sputtering conditions for the deposition of the above ZnO filsm are:

Pressure: 10μ

Gas Mixture: 20% O_2 + 80% A

Substrate Temp.: 200°C

Deposition Rate: 4μm/hour

Electrical Characteristics

After the ZnO film is deposited on the device structure, a set of Al inter-digital transducers is placed (by lift-off technique) on the free surface and the following tests can be carried out:

Insertion loss: Fig.10 shows the experimental setup for measuring the insertion loss of the delay line device. Fig.11 shows the X-Y recording of the filter response of one such device whose center frequency is located at 79.2 MHz where the loss is at a minimum of 56.5 db. The sidelobes appearing on this trace are due to harmonic wave excitations. The performance of this device is far from ideal. The theoretical limit of the insertion loss of any delay line employing ID transducers is 12 db, thus losses of 20-30 db is the desirable range for a practical device.

This measurement also provides a simple calculation of the surface acoustic wave velocity since

$$v = \lambda \cdot f = (60 \times 10^{-6} m)\ (79.2 \times 10^{6} sec^{-1})$$

$$= 4.75 \times 10^{3}\ m/sec$$

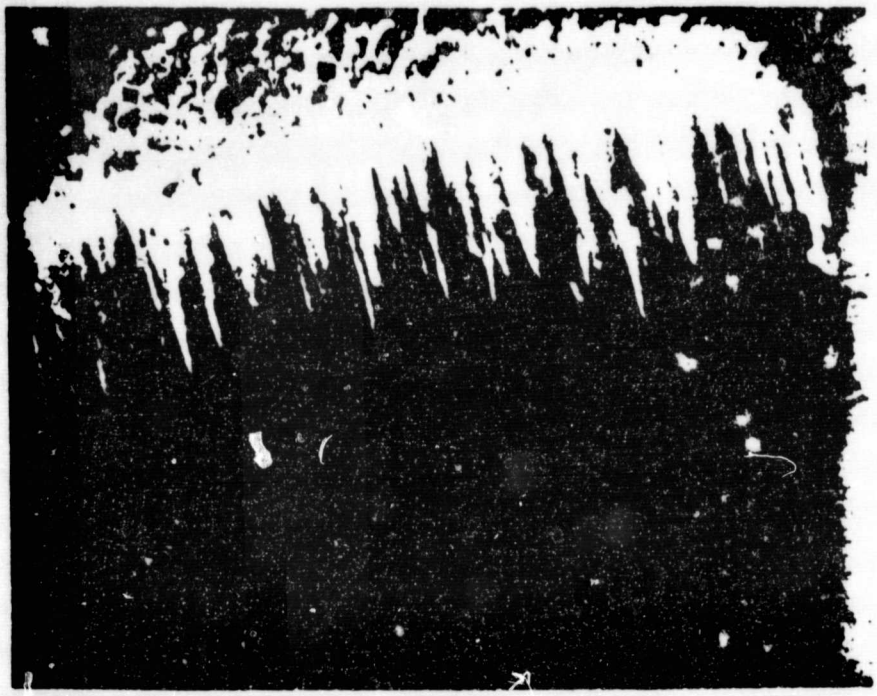

Fig. 9a. SEM photograph of ZnO sputtered on Au. Magnification is 160000X, viewing angle is 49°.

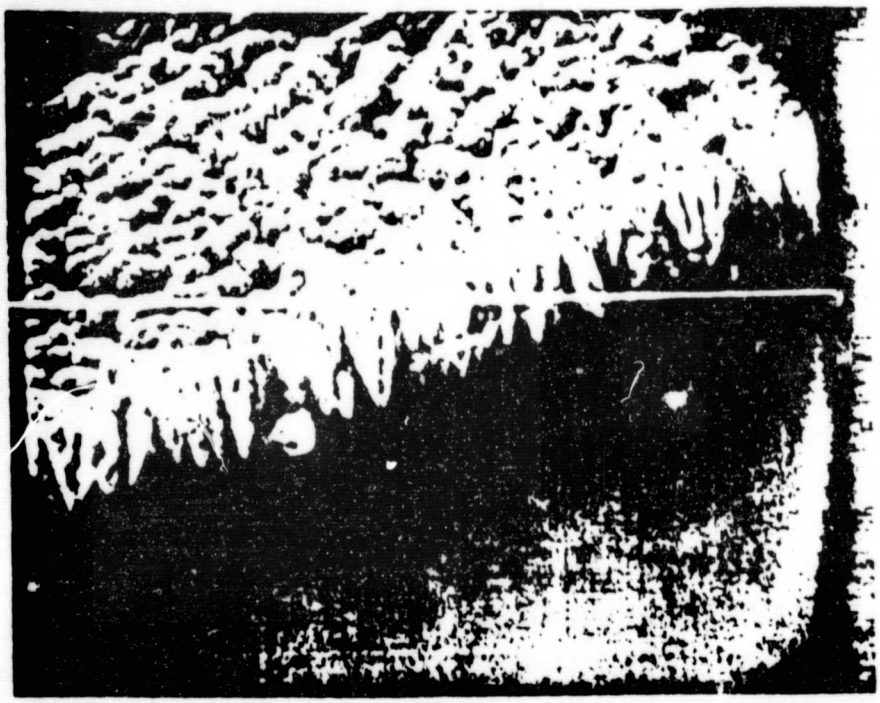

Fig. 9b. SEM photograph of ZnO film sputtered on Si. Magnification is 10000X, viewing angle is 45°

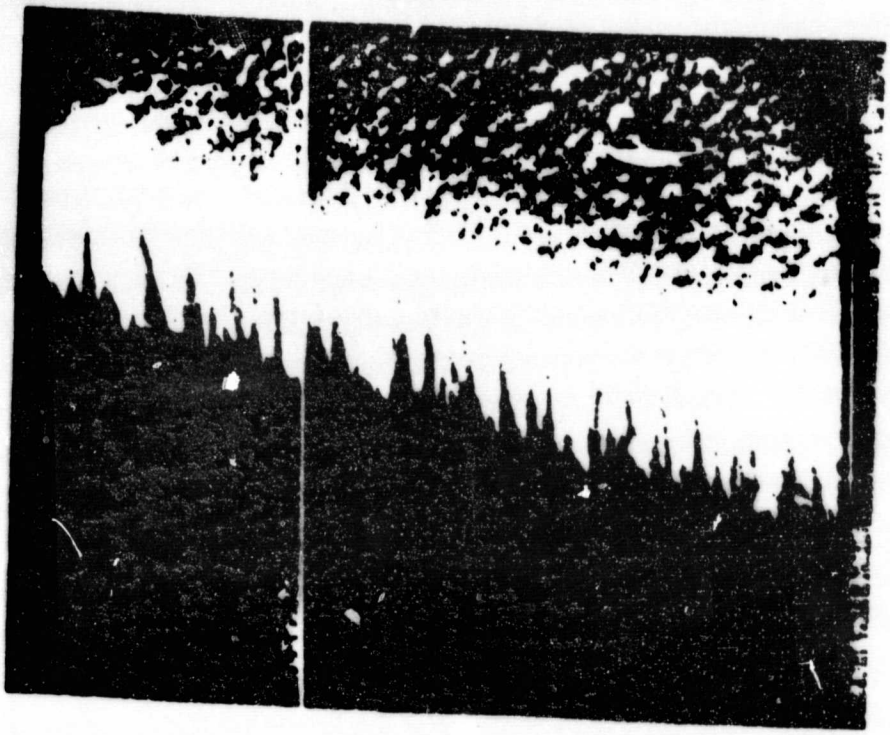

Fig 9c. SEM photograph of ZnO film sputtered on SiO_2. Magnification is 13600X, viewing angle is 45^{o}.

where $\lambda = 4 \cdot d = 60\,\mu m$ is the wavelength of the surface acoustic wave determined by the finger width d of the transducer. The finger width here is taken to be equal to the separation between consecutive fingers.

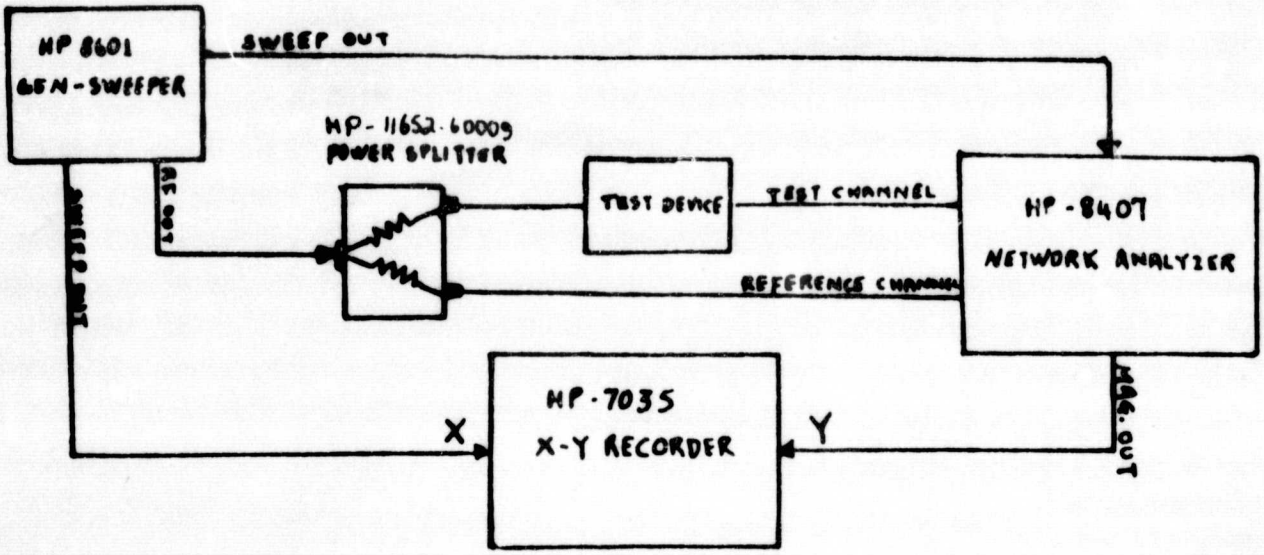

Fig. 10. Experimental setup for insertion loss measurement of a SAW device.

Delay time (τ) measurement:

Since the velocity of the surface acoustic wave is of the order of 10^5 cm/sec i.e. by a factor of 10^5 slower than the velocity of light, an electromagnetic signal can be delayed by an amount proportional to the separation of the two transducers.

The experimental setup for measuring the time delay of a SAW delay line is shown in Fig. 12. Fig. 13 shows an oscillograph of the input and output pulses of a delay line with 1.4 μsec delay. The input is a modulated pulse with carrier frequency equal to the resonant frequency of the transducer. This measurement provides another way of calculating the surface acoustic wave velocity from the expression

$$v = \frac{L}{\tau} = \frac{\text{transducer separation}}{\text{time delay}} = \frac{7 \times 10^{-3}\,m}{1.4 \times 10^{-6}\,sec}$$

$$= 5 \times 10^{3}\ cm/sec$$

for this particular device which has a 7 mm separation between the transducers.

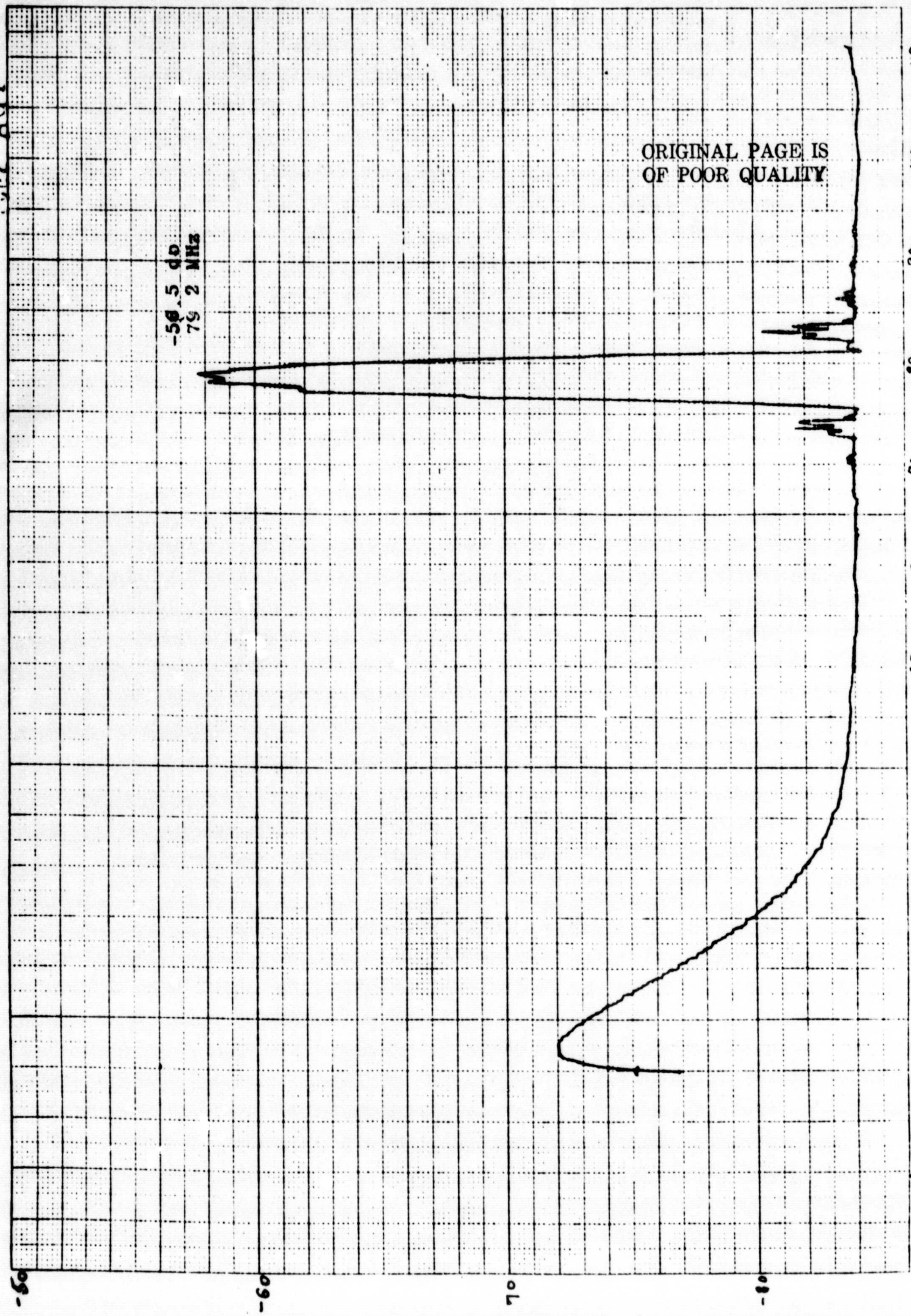

Figure 11. Frequency response of a SAW Filter.

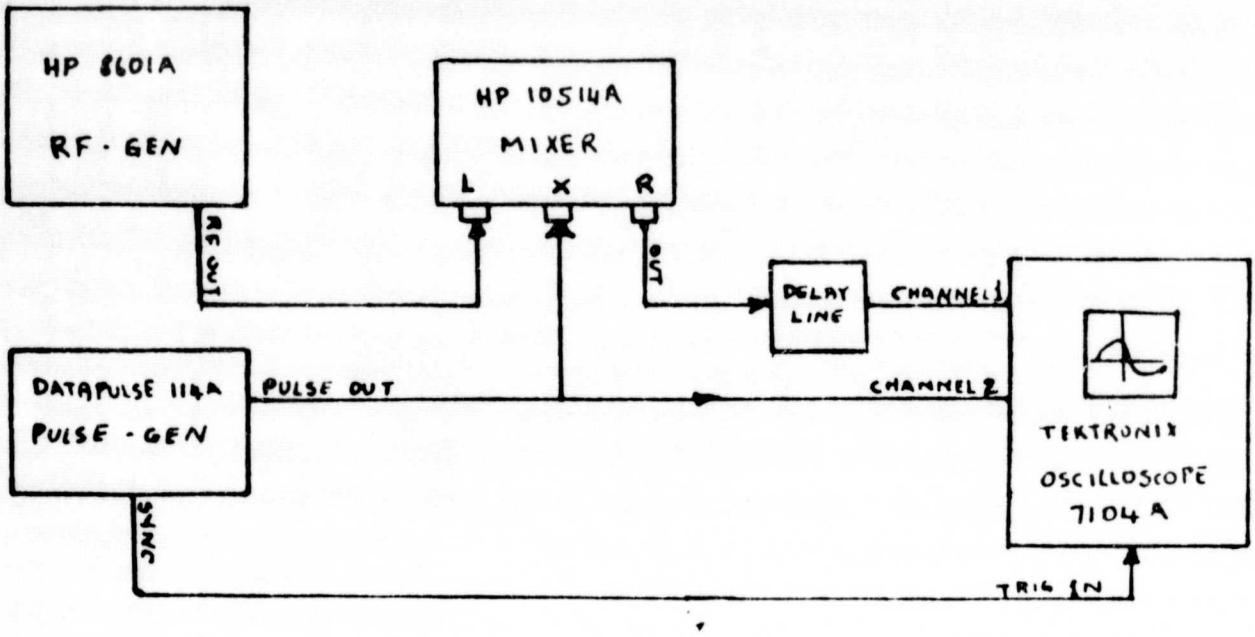

Fig 12. Experimental setup for time delay measurement of a SAW filter.

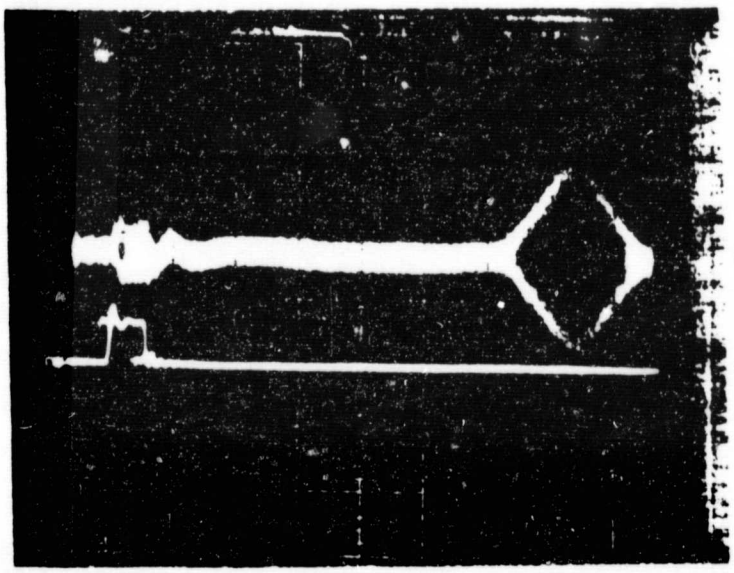

Ch. 1 delayed output

Ch. 2 input pulse

Fig 13. Oscillograph showing the delay characteristics of a SAW delay line.

Channel 1: 10 mV/div
Channel 2: .5 V/div

Horizontal scale: .2μsec/div